JOURNAL OF AIRCRAFT
Vol. 41, No. 3, May–June 2004

Engineering Notes

ENGINEERING NOTES are short manuscripts describing new developments or important results of a preliminary nature. These Notes cannot exceed 6 manuscript pages and 3 figures; a page of text may be substituted for a figure and vice versa. After informal review by the editors, they may be published within a few months of the date of receipt. Style requirements are the same as for regular contributions (see inside back cover).

Thermoelectric-Based Power System for Unmanned-Air-Vehicle/ Microair-Vehicle Applications

Jonathan Fleming* and Wing Ng†
Techsburg, Inc., Blacksburg, Virginia 24060
and
Saeid Ghamaty‡
Hi-Z Technology, Inc., San Deigo, California 92126

Introduction

THE microair-vehicle (MAV) research and development program was initiated by DARPA in the last half of the 1990s to determine the feasibility and usefulness of operating small microsized aircraft, primarily for military use. The adopted length scale range defined as micro was 15 cm (i.e., the aircraft should fit in a 15-cm square box) and is an order of magnitude smaller than any missionized unmanned air vehicle (UAV) currently operating.[§] One of the primary technical challenges facing MAVs is the development of small-scale propulsion and power systems with sufficient power density to provide necessary endurance and flight performance.[§] In almost all aircraft performance equations (maximum rate of climb, maximum endurance, range, etc.), weight is a key parameter. If the designer can reduce weight (especially dry weight), the aircraft performance will usually always benefit.[1]

One of the main sources of weight on a MAV vehicle designed for long-endurance missions are batteries—this is true even for an internal-combustion-powered aircraft. As an alternative to battery, a research program was initiated to investigate the use of lightweight, high-power-density thermoelectric generators for use as an onboard power system for MAV. A thermoelectric-generator (TEG) module is composed of a matrix of semiconductor material chosen for its thermoelectric properties—its ability to directly convert heat to electrical power with no moving parts. By converting waste heat to useful electric energy, significant weight savings can result.[2,3]

The use of TEGs as a power source for any vehicle hinges on the use of a heat engine (internal combustion, microturbine, etc.) as the primary propulsive energy source. As test results have shown, TEGs have been more effective on aircraft with larger power requirements, such as small rotary-wing vehicles or larger-scale fixed-wing aircraft—aircraft with power requirements of over 500 W. Note that the operating environment provided by the UAV is well suited for TEG operation: the heat source and cooling source are both provided by the propulsion system.

The primary goals and areas of research for this program were to 1) explore and investigate an innovative, lightweight approach of generating electric energy from waste heat energy through the use of thermoelectric modules and 2) develop new techniques for miniaturizing thermoelectric generator modules and to increase the power density (W/g) for applications to advanced miniature aircraft.

These research goals were successfully met, with benefits and drawbacks for TEG integration in MAVs identified. This Note documents the results based on this research program.

Module Development and Integration

TEG Module Development

In this research program, five different module types were developed and tested: the HZ-14, HZ-2, VHHFM-1, VHHFM-2, and VHHFM-2HE (high-efficiency version of the VHHFM-2). Figure 1 compares the relative sizes of the modules. All modules were fabricated of bismuth telluride and had nominal module efficiencies of 4.5%, except the VHHFM-2HE, which was about 6%. Module specifications are given in Table 1. Figure 2 shows the trend in increasing module power density with decreasing size.

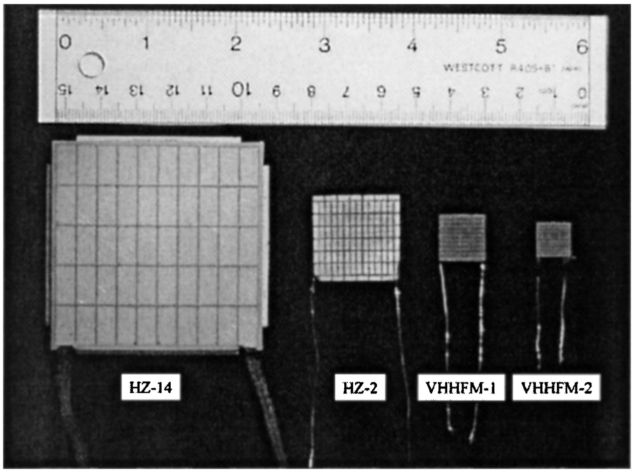

Fig. 1 Comparison of TEG modules. The VHHFM-2HE is the same physical size as the VHHFM-2.

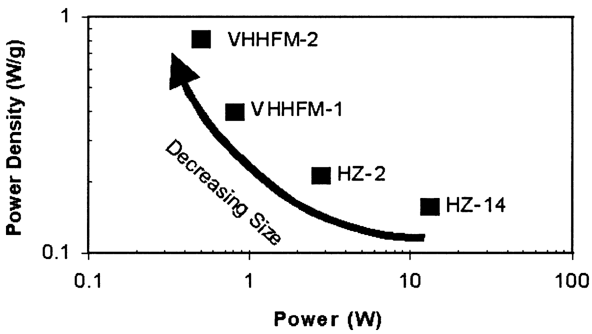

Fig. 2 Trend of TEG module power density increase with decreasing size. The power densities shown are maximum values obtained on a Seebeck tester.

Received 20 September 2002;

*Principal Research Engineer. Member AIAA.
†Chairman, 2901 Prosperity Road, Blacksburg, VA 24060. Associate Fellow AIAA.
‡Research Engineer.

§Data available online at http://www.darpa.mil/tto/MAV/mav_auvsi.html.

Table 1 Hi-Z TEG module specifications

	HZ-14	HZ-2	VHHFM-1	VHHFM-2	VHHFM-2HE
Size, thickness, cm	$6.3 \times 6.3 \times 0.51$	$2.9 \times 2.9 \times 0.51$	$1.3 \times 1.3 \times 0.2$	$1 \times 1 \times 0.2$	$1 \times 1 \times 0.2$
Weight, g	82	12.6	2.0	1.2	1.2
Design temp T_c, T_h, °C	30, 230	30, 230	30, 230	30, 230	30, 230
Design heat flux, W/cm^2	9.54	9.54	~24	~24	~24
Peak power, W	13	2.5	——	0.7–0.8	0.9
Peak efficiency	4.5%	4.5%	——	4.5–5.5%	6–6.5%

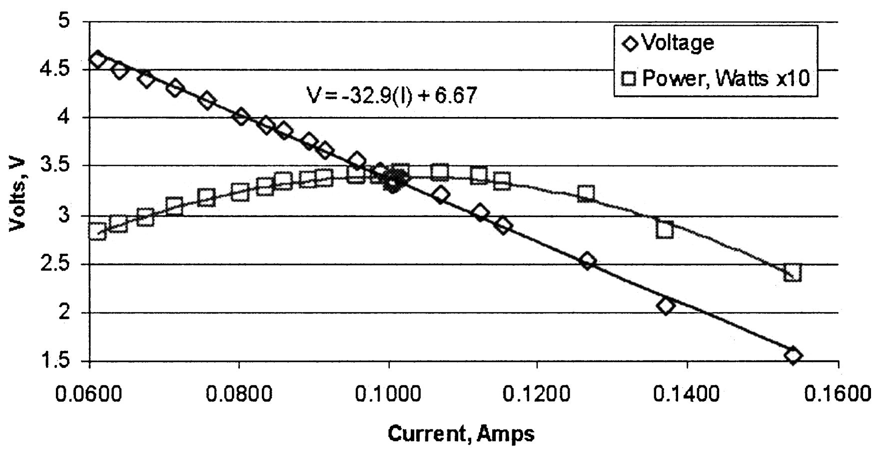

Fig. 3 Typical bench test results for a single TEG module test using the OS MAX 61 engine.

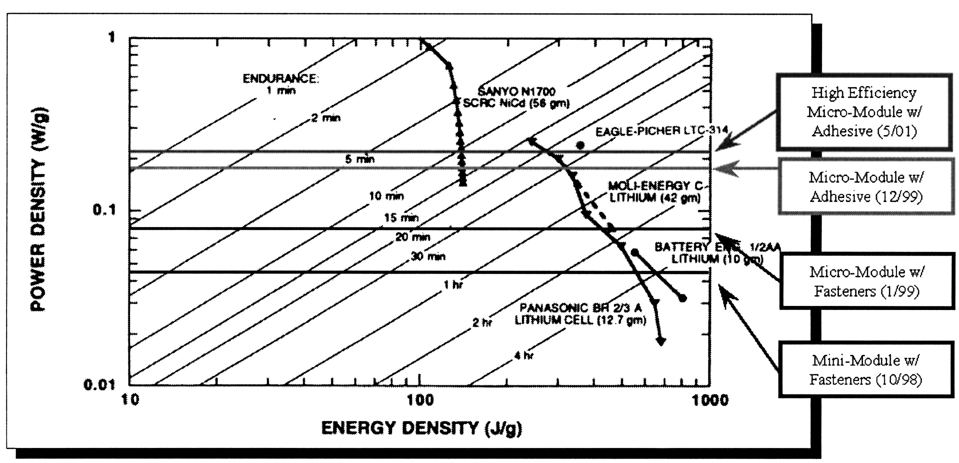

Fig. 4 History of installed TEG performance with OS 0.61 in.^{3} engine. Comparison to batteries is shown on this Ragone plot. (Battery data and Ragone plot from Ref. 4.)

After the TEG module was successfully miniaturized, module fabrication work focused on further improving the heat-flux conversion efficiency. This was achieved by improving the processing of the N-type material in the thermoelectric modules. The new version of the VHHFM-2, the VHHFM-2HE, exhibited a 20% performance increase over the existing modules.

TEG Module Integration and Testing

VHHFM-2 and VHHFM-2HE modules were the primary TEGs tested during this project. Several different small off-the-shelf model aircraft engines were used for testing: Cox 0.010 in.^{3}, Cox 0.049 in.^{3}, Norvell 0.061 in.^{3}, and OS MAX 0.61 in.^{3}

Different TEG mounting locations were used during testing, and it was found that the engine exhaust system offered the most mounting flexibility, access, and surface area for mounting compared to other options, such as the cylinder head. The thinner walls of the muffler also meant that a higher temperature gradient could be achieved across the TEG's thickness. For the engines tested, engine operating temperature typically increased with displacement. Exhaust gas temperatures of 150°C (Cox 0.010 in.^{3}) to 370°C (OS MAX 0.61 in.^{3}) were measured during testing. For a thermally efficient TEG integration design, approximately 40% of the total ΔT available ($T_{\mathrm{exhaust}} - T_{\mathrm{ambient}}$) could be used to generate power from the TEG modules. However, the exhaust gas temperatures were effected substantially by the engine's needle valve setting and overall condition.

Experimental Results

Experimental efforts progressed along two fronts: improving maximum integrated power output and power density through a series of bench tests and demonstrating more advanced TEG integration using proof-of-concept assemblies.

Key TEG Test and Performance Results

Much of the bench testing was done using the OS 0.61 in.^{3} engine. This engine was very convenient for testing because of its ease of setup (for module mounting) and its reliability and ease of operation.

Figure 3 shows a typical plot of output voltage and power vs system current for a VHHFM-2 module using the OS MAX 61 engine. Note the linear relationship between voltage and current and the resulting peak in power output when operating at matched-load conditions. Matched-load operation occurs when the load resistance equals the TEG module internal resistance. The absolute value of the slope of the voltage vs current curve is equal to the match-load resistance (in this case, approximately 33Ω).

The Ragone plot shown in Fig. 4 shows the history of the maximum installed power density for the VHHFM-2 modules with the OS MAX 61 engine. By the end of the research program, a maximum installed power density of 0.21 W/g had been achieved. Figure 4 also compares these results to different battery types, and the current break-even point of 20 min is clearly evident. Note, however, that this power output is at matched load conditions and maximum throttle setting for the engine.

The advances in power density are the result of increased power output through better module design and reduced TEG integrated assembly weight. The reduced weight is the main factor, and switching from mechanical fasteners and large heat exchanger assemblies to lightweight assemblies using adhesive and miniature heat exchangers resulted in more than 150% weight savings.

The optimum solution was found to be the use of lightweight aluminum heat exchangers (weighing fractions of a gram) along with a thermally conductive paste adhesive to hold the heat exchanger/module assembly together. A hot-side heat exchanger inserted into the muffler was usually always present as well.

Conclusions

In this research program, new high-temperature, high-efficiency microthermoelectric generator modules are developed and integrated onto unmanned microair-vehicle (MAV) propulsion systems. A $1 \times 1 \times 0.2$ cm module that produces up to 800 mW at a module thermoelectric efficiency of 6 to 7% (compared to 4% for commercially available modules) is demonstrated. The module is successfully integrated with small internal combustion engines used by developmental MAV vehicles. The maximum installed power output and power density for one of these miniature thermoelectric-generator modules was shown to be 380 mW and 210 mW/g, respectively. At this power density, TEGs outperform modern primary lithium batteries for system endurance requirements greater than 20 min.

Although there is still room for improvement, significant first steps were achieved during this research. One of the main innovations undertaken in this program was the development and integration of a small, high-performance TEG module into a system used outside of a laboratory setting. Although many advances in thermoelectric materials have been made in the past five years, little work has been performed in the area of practical research toward advanced applications of these materials outside of micropower applications. It is hoped that this work has contributed to the advancement of thermoelectric devices by focusing on the application of this technology to small-unmanned aircraft.

Acknowledgments

The work was sponsored by the Defense Advanced Research Projects Agency, Tactical Technology Office, under DARPA contract DABT63-98-C-0021 and is published with DARPA's approval. The authors would like to recognize and thank Samuel B. Wilson, III, and James McMichael of the Defense Advanced Research Projects Agency Tactical Technology Office who provided funding and guidance for this research.

References

[1] Anderson, J. D., Jr., *Introduction to Flight*, 3rd ed., McGraw–Hill, New York, 1989.

[2] Rowe, D. M. (ed.), *CRC Handbook of Thermoelectrics*, CRC Press, Boca Raton, FL, 1995.

[3] Angrist, S. W., *Direct Energy Conversion*, 3rd ed., Allyn and Bacon, Boston, MA, 1976.

[4] Johnson, D. C., "Micro Air Vehicle Missions and Technology Assessment," Lincoln Lab., Massachusetts Inst. of Technology, Project Rept. MAV-1, Lexington, MA, Nov. 1997.

Simple Trim Drag Prediction Method Based on the Biplane Theory

Kazuhiro Kusunose*
The Boeing Company, Seattle, Washington 98124-2207

Nomenclature

$\mathcal{R}_W, \mathcal{R}_{CW}, \mathcal{R}_{TW}$	=	aspect ratios defined by b_W^2/S_W, b_C^2/S_W, and b_T^2/S_W
b_W, b_C, b_T, b	=	spans of wing, canard, tail, and $\max(b_C, b_T)$
$C_D, C_{D\,\mathrm{ind}}, C_{D\,\mathrm{prof}}$	=	total, induced, and profile drag coefficients
$C_{D\,\mathrm{trim}}$	=	trim drag coefficient
$C_L, C_{LW}, C_{LC}, C_{LT}$	=	total, wing, canard, and tail lift coefficients
$C_{M\mathrm{cg}}, C_{MWB}$	=	defined by $M_{\mathrm{cg}}/qS_W\bar{c}$ and $M_{WB}/qS_W\bar{c}$ (Fig. 3)
$D, D_{\mathrm{ind}}, D_{\mathrm{prof}}$	=	total, induced, and profile drag
D_{ii}, D_{ij}	=	self- and mutually induced drag, $i, j = 1, \ldots, n$
e_W, e_C, e_T	=	Oswald's factors for wing, canard, and tail
L	=	total lift of the system
$L_{\mathrm{wing}}, L_{\mathrm{canard}}, L_{\mathrm{tail}}$	=	lifts of wing, canard, and tail
l_C, l_T	=	distances of canard and tail from c.g. (Fig. 3)
M_{cg}	=	net pitching moment about c.g. (Fig. 3)
M_{WB}	=	wing–body pitching moment, $-L_{\mathrm{wing}}(x_W - x_{\mathrm{cg}})$
q	=	freestream dynamic pressure, $\rho_\infty U_\infty^2/2$
$S_W, \bar{c}$	=	wing reference area and wing reference chord
X, Y	=	defined in Eqs. (20) and (21)
x_W, x_{cg}	=	locations of center of pressure (wing–body) and c.g.
σ	=	interference factor (Ref. 1)

Introduction

FOR an airplane to fly with longitudinal equilibrium, it must be trimmed; the net pitching moment acting on the c.g. of the airplane must be zero. In the present analysis, we define the trim drag as the necessary induced drag penalty, or cost to the airplane of being trimmed. Classic biplane theory[1,2] is used to estimate the induced drag of multiwing configuration systems.[3,4] One obvious problem in trimming three-wing configurations is that there exist an infinite number of three-wing loading combinations that will trim the pitching moment of the system. Meredith,[4] at The Boeing Company, developed an approximation method for optimally trimming three-wing configurations. The main purpose of this engineering Note is to extend Meredith's approximation method[4] and develop a general trim-optimization method for three-wing configurations.

Discussion

According to the Helmholtz vortex theorems, the "bound vortex" of a wing cannot end at the wing tips but must continue on infinitely

Received 27 October 2003; presented as Paper 2004-0901 at AIAA 42nd Aerospace Sciences Meeting and Exhibit, Reno, NV, 5–8 January 2004; revision received 16 January 2004; accepted for publication 17 January 2004.

*Research Engineer, Acoustics and Fluid Mechanics, P.O. Box 3707, MC 67-LF; kazuhiro.kusunose@boeing.com. Member AIAA.